White Blood Cell Count Shape Heart-Brain Coupling and rTMS Benefit in Depression

Bruno Pedraz-Petrozzi[1,2,3,4,*], Jonas Wilkening[5], Alexander Sartorius[1,2,4], Martijn Arns[6,7], Roberto Goya-Maldonado[5]

[1]Department of Psychiatry and Psychotherapy, Central Institute of Mental Health, Medical Faculty Mannheim, University of Heidelberg, Mannheim, Germany.
[2]German Center for Mental Health (DZPG), partner site Mannheim, Germany.
[3]Research Group of Stress-related Disorders, Department of Psychiatry and Psychotherapy, Central Institute of Mental Health, Clinical Faculty Mannheim, University of Heidelberg, Mannheim, Germany.
[4]Research Group Brain Stimulation, Department of Psychiatry and Psychotherapy, Central Institute of Mental Health, Clinical Faculty Mannheim, University of Heidelberg, Mannheim, Germany.
[5]Laboratory of Systems Neuroscience and Imaging in Psychiatry (SNIP-Lab), Department of Psychiatry and Psychotherapy, University Medical Center Göttingen, Göttingen, Germany.
[6]Brainclinics Foundation, Nijmegen, The Netherlands.
[7]Stanford Brain Stimulation Lab, Stanford University, Palo Alto, United States of America.

[*]Corresponding author:
Dr. Bruno Pedraz-Petrozzi, Ph.D.
Central Institute of Mental Health (CIMH)
Department of Psychiatry and Psychotherapy
J5
D-68159 Mannheim
Germany
Phone: +49 621 1703 4363
Email: bruno.pedraz@zi-mannheim.de
ORCID: 0000-0002-4119-971X

Authors' ORCID:
Martijn Arns, ORCID: 0000-0002-0610-7613
Roberto Goya-Maldonado, ORCID: 0000-0002-7368-1332
Alexander Sartorius, ORCID: 0000-0002-1243-3693
Jonas Wilkening, ORCID: 0009-0000-3539-1900

Abstract Word Count: 149 words
Total Word Count: 2998 words

Keywords (MeSH terms): Major Depressive Disorder; Inflammation; rTMS; iTBS; Leukocytes; Heart-Brain Coupling; Biomarkers; Treatment Response.

Ethics Approval and Consent to Participate: The study protocol (https://clinicaltrials.gov/study/NCT05260086) was conducted in accordance with the

Declaration of Helsinki and approved by the Ethics Committee of the University Medical Center Göttingen (UMG). All participants provided both verbal and written informed consent after receiving a full explanation of the study procedures.

Consent for Publication: Not applicable.

Availability of Data and Materials: The data supporting the findings of this study are not publicly available due to European Union data protection regulations. However, data may be made available upon reasonable request from the corresponding author, provided appropriate legal and ethical conditions are met.

Competing Interests: The authors declare no competing interests.

Funding: This project received financial support from the German Federal Ministry of Education and Research (*Bundesministerium für Bildung und Forschung*, BMBF: 01 ZX 1507, "PreNeSt - e:Med''). The funders had no role in the study design, data collection, analysis, interpretation, or manuscript preparation.

Employment: None of the authors was employed or contracted by any organization that could gain or lose financially from the publication of this manuscript.

Acknowledgements: This work was supported by the German Federal Ministry of Education and Research (*Bundesministerium für Bildung und Forschung*, BMBF: 01 ZX 1507, "PreNeSt - e:Med'').

Personal Financial Interests: The authors did not receive any form of financial compensation (e.g., salaries, stocks, consulting fees) from commercial entities related to this research.

Statement: During the preparation of this manuscript, the authors used Grammarly Inc. and ChatGPT to assist with language refinement and grammar correction. Elicit was used to support the literature search. All content was critically reviewed and edited by the authors, who take full responsibility for the final version of the manuscript.

Declarations of Interest: BP-P acknowledges receiving a Seed Money for Research grant from the Central Institute of Mental Health. RG-M acknowledges receiving a grant from the German Federal Ministry of Education and Research (*Bundesministerium für Bildung und Forschung*, BMBF: 01 ZX 1507, "PreNeSt - e:Med''). MA holds equity/stock in Sama Therapeutics, served as consultant to Synaeda, Sama Therapeutics, Neumarker and is named inventor on patents and intellectual property but receives no royalties.

ABSTRACT

Low-grade inflammation affects approximately 30% of individuals with major depressive disorder (MDD) and has been associated with poorer treatment outcomes, reduced antidepressant response, autonomic dysregulation, and increased cardiometabolic risk. This inflammatory state may contribute to variability in response to intermittent theta burst stimulation (iTBS) over the left dorsolateral prefrontal cortex. In this study, inflammation was indexed by clinical routine markers white blood cell count (WBC) and C-reactive protein (CRP), while heart-brain coupling (HBC), a physiological marker of frontal-vagal engagement, was derived from electrocardiographic data during the first iTBS sessions. Higher HBC was associated with symptom improvement only in individuals with lower WBC. Diffusion MRI revealed elevated free-water in the fornix and corpus callosum in patients with higher WBC, suggesting a neuroimmune profile linked to reduced clinical benefit. These findings indicate that baseline inflammation shapes the clinical relevance of HBC and may help explain variability in iTBS efficacy.

INTRODUCTION

Over the past decade, repetitive transcranial magnetic stimulation (rTMS) has emerged as a non-invasive treatment for major depressive disorder (MDD) resistant to first-line antidepressants[1]. Intermittent theta burst stimulation (iTBS), a patterned rTMS protocol targeting the left dorsolateral prefrontal cortex[2], achieves efficacy comparable to conventional rTMS with shorter sessions (e.g., Blumberg and colleagues[3]). Yet clinical outcomes remain highly variable[4], highlighting the need for biomarkers of target engagement and moderators of treatment response.

Low-grade inflammation, defined as subclinical elevation of inflammatory mediators as white blood cell count (WBC) and C-reactive protein (CRP) in the absence of acute infection[5], can occur in ~30% of MDD patients[6]. It has been associated with worse clinical outcomes, reduced antidepressant response, autonomic imbalance, and increased cardiometabolic risk[7–11]. Systemic inflammation may also parallel central changes such as microglial activation, vasogenic edema, and extracellular matrix disruption, increasing extracellular water content in neural tissue[12,13]. Diffusion MRI free-water (FW) fraction is a sensitive, non-invasive marker of this extracellular component[14–16] and correlates with peripheral inflammation in depression[12,13]. Preclinical evidence further indicates that vagal stimulation can reduce neuroinflammatory cascades and tissue edema [17–20].

Emerging models highlight the DLPFC's role within a frontal-vagal network linking cortical and autonomic regulation[21,22]. Heart-brain coupling (HBC), defined as synchronization of cardiac rhythms with stimulation trains, has been proposed as a physiological marker of iTBS-induced vagal engagement[23]. While robust HBC reflects neural-autonomic engagement, the conditions under which this coupling is shaped remain unclear. The vagus nerve plays a central role in regulating immune responses through its anti-inflammatory reflex[24], suggesting that baseline inflammation may influence vagal activity. In this context, routine clinical markers such as WBC and CRP offer distinct but complementary indices of immune tone. WBC reflects circulating immune activity, whereas CRP represents an acute-phase hepatic response[25]. Both predict adverse outcomes and are accessible, low-cost tools for stratifying patients [26]. Compared to cytokines, they can be measured easily at baseline, enabling translational application.

In this study, we tested whether baseline inflammation moderates the prognostic value of HBC in MDD patients undergoing iTBS. Specifically, we examined whether WBC or CRP moderated the association between HBC and treatment response, and whether corresponding FW alterations reflected neuroinflammatory signatures. We hypothesized that these routine clinical markers would serve as a sensitive index of immune tone, and that elevated inflammation would be associated with increased FW in tracts linked to affective regulation, particularly in limbic and prefrontal pathways implicated in affective and autonomic regulation, reflecting reduced benefit to iTBS.

RESULTS

WBC - But Not CRP - Shapes HBC And iTBS Clinical Benefit

We first examined whether systemic inflammation moderated the relationship between HBC during stimulation and clinical response in our general sample (**Table 1; see column "full sample"**). Two logistic regression models were tested, each including treatment condition (active vs. sham), mean-centered HBC (HBCc), one inflammatory marker (WBCc or CRPc), and their interaction.

The WBC model showed good fit (AIC = 65.1; McFadden's R^2 = 0.18; Nagelkerke's R^2 = 0.27) and revealed a significant interaction between HBCc and WBCc (χ^2 = 6.96, p = 0.008), as well as a main effect of treatment (χ^2 = 5.81, p = 0.016). HBCc and WBCc alone were not significant predictors. Parameter estimates confirmed the interaction (OR = 0.51, 95% CI [0.27, 0.86], p = 0.023), indicating that the association between HBC and response weakened with increasing WBC. Active stimulation was associated with higher response likelihood (OR = 6.48, 95% CI [1.39, 41.93], p = 0.028). As shown in **Figure 1a**, HBC was positively associated with response at low WBC, but not at average or high levels.

Bootstrap validation (B = 1000, BCa) supported this pattern. The HBCc × WBCc interaction remained significant (OR = 0.23, 95% CI [0.19, 0.83], p = 0.002), and WBCc alone emerged as a negative predictor (OR = 0.32, 95% CI [0.24, 0.97], p = 0.014). HBCc was again non-significant (OR = 2.11, p = 0.286), while active treatment remained predictive of response (OR = 132.98, 95% CI [0.98, 219.59], p = 0.036). Model performance remained stable (McFadden's R^2 = 0.25; Nagelkerke's R^2 = 0.34). These findings indicate that elevated inflammation, as indexed by WBC, weakens the clinical relevance of HBC.

By contrast, substituting CRPc yielded a weaker model (AIC = 74.4; McFadden's R^2 = 0.04), with no significant interaction between HBCc and CRPc (χ^2 = 0.09, p = 0.77), and no main effects for CRPc or treatment (**Table 2**).

Table 1 - Sample characteristics and subgroup comparisons by baseline WBC. Continuous variables are shown as mean (SD), and categorical variables as percentages or proportions. P-values reflect t-tests or Fisher's exact tests for the subgroups' columns "lower-WBC" and "higher-WBC," as appropriate. Abbreviations: MADRS = Montgomery-Åsberg Depression Rating Scale; HBC = heart-brain coupling; WBC = white blood cell count; CRP = C-reactive protein; TRD = treatment-resistant depression; AD = antidepressants; SSRI = selective serotonin reuptake inhibitors; W = week.

Variable	Full Sample	Lower-WBC	Higher-WBC	p-value(t / Fisher)
Sample	64	24	40	
Age (years)	36.05 (13.49)	36.54 (13.39)	35.75 (13.70)	0.822
Sex, male (%)	56.30% (36)	66.70% (16)	50.00% (20)	**0.298**
Group allocation				
Active stimulation (%)	48.40% (31)	33.30% (8)	57.50% (23)	**0.075**
Sham stimulation (%)	51.60% (33)	66.70% (16)	42.50% (17)	
Averaged HBC	-0.74 (1.41)	-1.05 (1.19)	-0.56 (1.51)	0.176
CRP (mg/L)	1.78 (2.04)	1.38 (1.88)	2.02 (2.12)	0.023
WBC ($\times 10^9$/L)	6.97 (1.47)	5.51 (0.64)	7.85 (1.05)	-
MADRS Score				
Baseline (Week 1)	22.75 (6.60)	22.79 (6.51)	22.73 (6.74)	0.969
Week 3	17.59 (8.77)	17.21 (10.73)	17.82 (7.49)	0.788
% Change (W1-W3)	-18.05 (54.48)	-25.07 (40.92)	-13.83 (61.31)	0.429
Treatment Response (%)	21.90% (14/64)	25.00% (6/24)	20.00% (8/40)	**0.757**
TRD (%)	37.50% (24/64)	37.50% (9/24)	37.50% (15/40)	**1.000**
Medication Category				
None	31.30% (20)	25.00% (6)	35.00% (14)	**0.251**
Not antidepressant	4.70% (3)	8.30% (2)	2.50% (1)	
Other AD (non-SSRI)	34.40% (22)	45.8% (11)	27.50% (11)	
SSRI	29.70% (19)	20.80% (5)	35.00% (14)	

Table 2 - Parameter estimates of the logistic regression model for WBC and CRP. Abbreviations: WBCc = (mean-centered) white blood cell count; HBCc = (mean-centered) heart-brain coupling.

WBC

	B ± SE	z	p	OR [95 % CI]
Active vs. Sham	**1.87 ± 0.85**	**2.20**	**0.028**	**6.48 [1.39, 41.93]**
HBCc	0.23 ± 0.25	0.93	0.350	1.26 [0.77, 2.12]
WBCc	-0.55 ± 0.32	-1.72	0.086	0.58 [0.28, 1.02]
HBCc × WBCc	**-0.67 ± 0.29**	**-2.28**	**0.023**	**0.51 [0.27, 0.86]**

CRP

	B ± SE	z	p	OR [95 % CI]
Active vs. Sham	0.75 ± 0.64	1.17	0.243	2.12 [0.62, 7.96]
HBCc	0.16 ± 0.27	0.58	0.561	1.17 [0.70, 2.08]
CRPc	-0.07 ± 0.17	-0.41	0.682	0.93 [0.62, 1.26]
HBCc × WBCc	-0.06 ± 0.20	-0.30	0.762	0.94 [0.66, 1.51]

HBC Benefits Emerge Only at Lower WBC Levels

To further characterize the WBC × HBC interaction, we conducted simple-slope and Johnson-Neyman analyses. At one standard deviation below the mean WBC (≈5.5 × 10^9/L), higher HBC was significantly associated with clinical response (B = 1.21 ± 0.49, p = 0.014), corresponding to an approximate threefold increase in odds (OR ≈ 3.35). This association was nonsignificant at average WBC (≈6.97 × 10^9/L) and reversed direction, though not significantly, at one standard deviation above the mean (≈8.4 × 10^9/L; B = -0.74 ± 0.50, p = 0.14).

Johnson-Neyman analysis (**Figure 1b**) identified a critical threshold at WBCc = -0.53 (≈6.44 × 10^9/L), below which HBC was positively associated with response. This lower-inflammation subgroup comprised 24 of 64 participants (38%). At the high end of the WBC range (≈10.7 × 10^9/L), only one participant was represented, limiting interpretability in this range.

Average and Conditional Marginal Effects Across WBC Levels

To examine how treatment and HBC influenced response across inflammation levels, we analyzed average and conditional marginal effects. On average, active stimulation increased the probability of clinical response by 25.3 percentage points (p = 0.010), while each standard deviation increases in WBC reduced response likelihood by 9.3 points (p = 0.021). HBC alone showed no significant main effect after accounting for treatment and inflammation (**Table 3**).

Conditional marginal effects clarify this interaction more (**Table 4**). At low WBC (≈5.5 × 10^9/L), active treatment increased response probability by 30.4 points (p = 0.014), with HBC contributing an additional 13.6 points (p = 0.001). At average WBC (≈6.97 × 10^9/L), the treatment effect remained significant (+27.1 points, p = 0.016), but HBC added little (+3.4 points, p = 0.346). At high WBC (≈8.4 × 10^9/L), treatment benefit was attenuated (+19.7 points, p = 0.026), and HBC slightly reversed direction (-4.7 points, p = 0.246). WBC had a significant negative effect only below or at the mean.

Table 3 - Average Marginal Effects. Abbreviations: AME = average marginal effects, SE = standard error; WBCc = (mean-centered) white blood cell count; HBCc = (mean-centered) heart-brain coupling.

	AME	**SE**	***z***	***p***	**95 % CI**
Active vs sham	0.253	0.10	2.56	0.010	[0.06, 0.45]
HBCc	0.054	0.03	1.59	0.111	[-0.01, 0.12]
WBCc	-0.093	0.04	-2.31	0.021	[-0.17, -0.01]

Table 4 - Conditional Marginal Effects at WBCc levels. Abbreviations: AME = average marginal effects, SE = standard error; WBCc = (mean-centered) white blood cell count; HBCc = (mean-centered) heart-brain coupling.

	WBCc	**AME**	**SE**	***z***	***p***	**95 % CI**
Active vs sham	-1 SD	0.304	0.12	2.46	**0.014**	[0.06, 0.55]
	Mean	0.271	0.11	2.42	**0.016**	[0.05, 0.49]
	+1 SD	0.197	0.09	2.22	**0.026**	[0.02, 0.37]
HBCc	-1 SD	0.136	0.04	3.29	**0.001**	[0.05, 0.22]
	Mean	0.034	0.04	0.94	0.346	[-0.04, 0.10]
	+1 SD	-0.047	0.04	-1.16	0.246	[-0.13, 0.03]
WBCc	-1 SD	-0.112	0.05	-2.44	**0.015**	[-0.20, -0.02]
	Mean	-0.110	0.05	-2.28	**0.023**	[-0.21, -0.02]
	+1 SD	-0.035	0.04	-1.00	0.317	[-0.11, 0.03]

HBC Shows Discriminative Value Only Under Lower Inflammation

To assess whether inflammation modulated the discriminative utility of HBC, we computed ROC curves in two subgroups defined by WBCc. The sample (n = 64) was split at the Johnson-Neyman threshold (WBCc = -0.53; ≈6.44 × 10^9/L), yielding a lower-WBC group (n = 24; mean WBC: 5.51 ± 0.64) and a higher-WBC group (n = 40; mean WBC: 7.85 ± 1.05). Log-transformed CRP was significantly elevated in the higher-WBC group (t(62) = -2.34, p = 0.023), supporting the biological validity of this stratification. Additionally, 75% of higher-WBC participants met criteria for low-grade inflammation (CRP > 3 mg/L), compared to 25% in the lower-WBC group. More descriptive information about the two subgroups is illustrated in **Table 1 (see columns "lower-WBC" and "higher-WBC")**.

In the lower-inflammation subgroup, HBC demonstrated clear discriminative ability (AUC = 0.78, 95% CI [0.56, 0.99]). At the optimal threshold (HBCc ≥ 0.69; raw HBC ≈ -0.05), classification accuracy reached 83% (67% sensitivity, 89% specificity), distinguishing two-thirds of individuals with ≥50% MADRS reduction while misclassifying only 11% of those without such improvement. In contrast, HBC failed to distinguish responders in the higher-WBC group (AUC = 0.52, 95% CI [0.29, 0.74]); the ROC curve approximated chance, with poor classification performance (38% sensitivity, 41% specificity, 40% accuracy). Although average HBC values did not differ between low- and high-WBC participants (t(62) = -1.37, p = 0.176), ROC analyses revealed that HBC discriminated responders from non-responders only in the low-WBC group, whereas classification performance was at chance in the high-WBC group. As shown in **Figure 1c**, only the lower-WBC group exhibited meaningful separation of outcome based on HBC.

Associations Between WBC and White Matter Free-Water (FW) from DTI

To examine whether inflammation-related differences in HBC were mirrored in white matter microstructure, we conducted diffusion MRI connectometry using subgroups defined by the WBC × HBC interaction. As in the ROC analysis, participants were split at the Johnson-Neyman threshold into lower- and higher-WBC groups. Parametric correlations between FW and WBC were assessed within each group, and an exploratory analysis directly compared the two.

In the lower-WBC subgroup, WBC was positively associated with increases in white matter FW. The robust effects were observed in the fornix and corpus callosum (forceps major and tapetum), with additional contributions from the thalamic radiation. No negative associations were detected. In contrast, the higher-WBC group showed a more heterogeneous pattern, including both positive and negative correlations. Positive associations clustered in the forceps major, tapetum, and fornix, with smaller contributions from thalamic and occipital tracts. Negative correlations were confined mainly to the fornix and tapetum. Full tract counts and proportions are provided in Supplementary Material 1. Representative streamlines are shown in **Figure 1d**.

Direct comparison between higher- and lower-WBC groups revealed 184 tracts with significantly higher FW values in the higher-WBC subgroup, particularly in the right fornix and body of the corpus callosum (**Figure 1e**). These were primarily localized to the right fornix and the body of the corpus callosum, with additional effects in the left fornix, tapetum, and right anterior thalamic radiation (ATR).

Together, these findings indicate that systemic inflammation is associated with distinct patterns of microstructural white matter alterations. In lower-WBC individuals, FW increases were widespread and anatomically coherent, converging on limbic and interhemispheric pathways. In contrast, higher-WBC individuals showed fragmented effects, including local reductions in FW. These structural patterns parallel the physiological findings, suggesting that inflammation may constrain both neurocardiac engagement and underlying brain network flexibility.

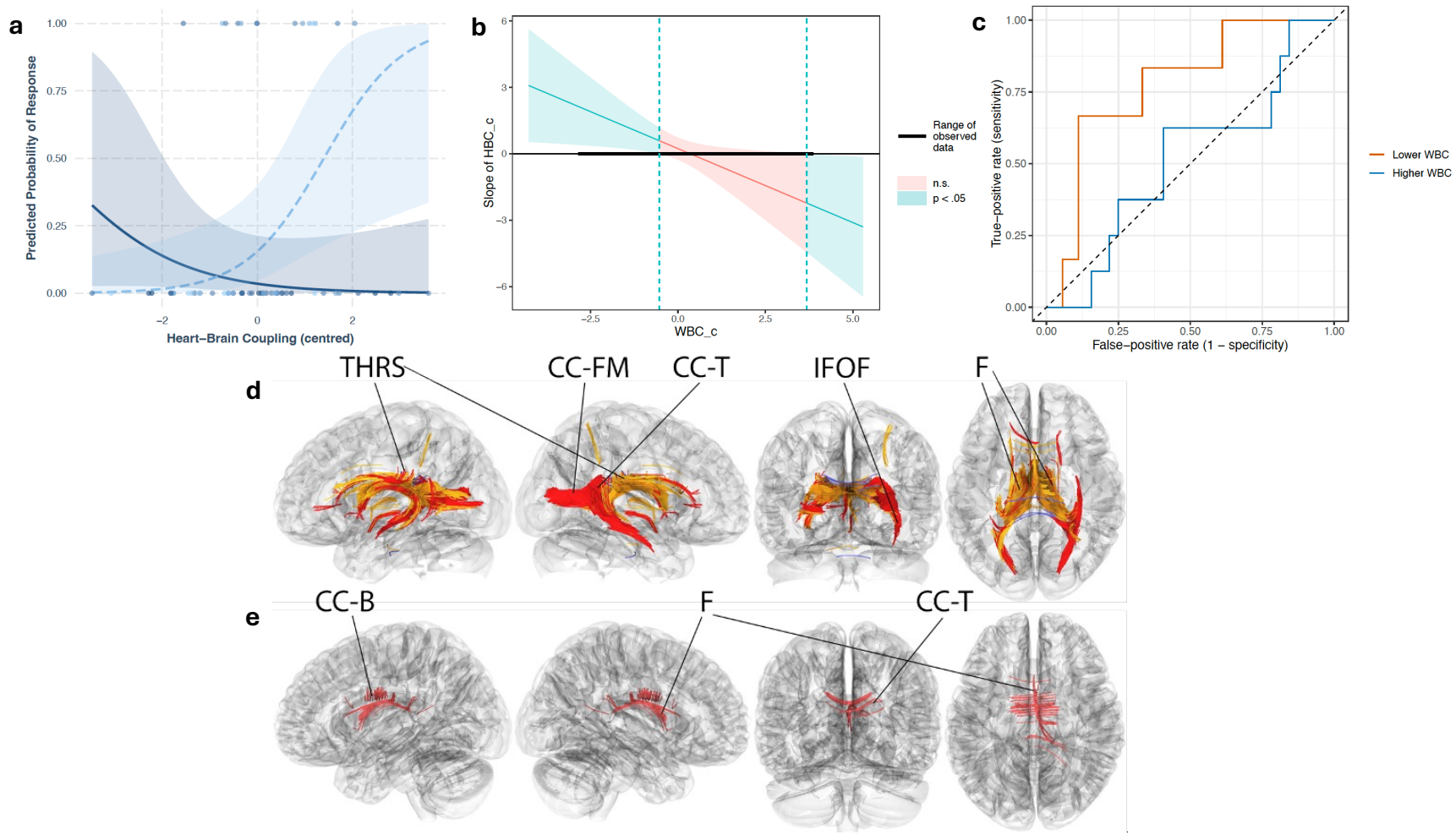

Figure 1. White blood cell count (WBC) moderates the relationship between heart-brain coupling (HBC), clinical response, and free-water (FW) white matter tracts.

a) Moderation of the relationship between centered heart-brain coupling (HBC_c) and clinical response by baseline leucocyte count (WBC_c). Solid line = higher inflammation (+1 SD WBC); dashed line = lower inflammation (-1 SD). Shaded ribbons represent 95% confidence intervals. Jittered dots denote individual responders (y = 1) and non-responders (y = 0). The crossover demonstrates that higher HBC is associated with response only at lower inflammation levels. b) Johnson-Neyman plot showing the region of significance for the mean-centered HBC; response slope as a function of mean-centered baseline WBC. c) Receiver operating characteristic (ROC) curves for classifying clinical response based on HBC, stratified by baseline WBC: lower inflammation (WBCc < -0.53; orange) and higher inflammation (WBCc ≥ -0.53; blue). Each curve shows sensitivity versus 1 - specificity across HBC thresholds. d) Correlational tractography results showing tracts where free-water (FW) correlated with WBC in each subgroup: positive (red) and negative (blue) correlations in the high-WBC group, and positive correlations (orange) in the low-WBC group. e) Correlational tractography results from the direct group comparison. Tracts in red show higher FW in the higher-WBC group compared to the lower-WBC group.

Abbreviations: WBCc = mean-centered white blood cell count; HBCc = mean-centered heart-brain coupling; FW = free-water; CC-B = corpus callosum (body); CC-FM = corpus callosum (forceps major); CC-T = corpus callosum (tapetum); F = fornix; IFOF = inferior fronto-occipital fasciculus; THRS = thalamic radiation, superior.

DISCUSSION

Our study found that the therapeutic benefits of HBC during iTBS varied depending on the patient's baseline immune tone. In our sample, higher HBC levels were linked to clinical improvement only in patients with lower systemic inflammation, as measured by WBC count. However, when WBC was higher, HBC provided little benefit and may even have been detrimental. This finding was supported by ROC analyses and confirmed by diffusion MRI, which showed increased FW in key white matter tracts among patients with higher WBC, indicating central neuroinflammation. These results suggest that inflammation is a boundary condition for effective neuromodulation.

The main findings of this study identify WBC, a routine clinical marker, as a key moderator of the relationship between HBC and treatment response during iTBS in MDD. Notably, baseline clinical and demographic characteristics (including age, sex, treatment allocation, medication type, symptom severity, and HBC) did not significantly differ between the lower- and higher-WBC groups, suggesting that the observed moderation effect is unlikely to be explained by these variables alone. To our knowledge, no prior studies have reported a moderating effect of inflammatory parameters on autonomic activity (such as HBC) during iTBS. Interpreting this result requires consideration of vagal physiology. HBC reflects vagal activation via the frontal-vagal pathway in the context of rTMS[21], involving coordinated interactions between the DLPFC and subgenual anterior cingulate cortex[21,27]. This circuit plays a critical role in regulating both affective and autonomic functions[21,27]. Increased vagal tone, through parasympathetic activation and the cholinergic anti-inflammatory pathway[28–30], is not only essential for cardiac rhythm regulation but also contributes to immune modulation by promoting anti-inflammatory responses[28,29,31,32]. For example, studies using vagus nerve stimulation in individuals with depression have demonstrated reductions in pro-inflammatory cytokines, underscoring the vagus nerve's immunomodulatory capacity[33]. In line with this, high resting vagal tone, as indexed by HRV, has been associated with lower levels of CRP and WBC[34,35]. Animal studies further support this link, showing that vagal stimulation reduces sympathetic activity and modulates leukocyte distribution[36]. Conversely, reduced vagal activity is associated with impaired immune regulation, elevated inflammatory states, lower HRV, and, in some cases, increased risk of mortality[31,34] and chronic disease[37].

In contrast, CRP did not moderate the relationship between HBC and treatment response in our data, though this null finding should be interpreted with caution. CRP reflects hepatic acute-phase activity[25] and is primarily regulated by IL-6[38], but may not directly capture the dynamic immune-autonomic interactions indexed by WBC[28,29,33]. The autonomic system can influence leukocyte mobilization and adhesion[39,40], processes not directly reflected in CRP levels. Additionally, CRP exists in isoforms with divergent effects (pentameric CRP is anti-inflammatory, while monomeric CRP is pro-inflammatory[38]) and its higher interindividual variability may reduce sensitivity to subtle baseline immune differences[41]. Although our data

suggest a limited role for CRP in this context, larger or multimodal studies may yet detect associations not observable here.

Depression has been linked with changes in cardiac activity, immune function, and increased overall health risks[42]. People with depression are more likely to develop cardiovascular diseases[43], which can lead to longer hospital stays and a more difficult illness progression[44]. Lower heart rate variability, a sign of autonomic nervous system imbalance, frequently occurs in these individuals[45]. In about 30% of cases[6], low-level chronic inflammation is present, and this inflammation can contribute independently to cardiovascular disease[46]. These factors together may increase overall health challenges. Research also shows that higher inflammation and lower heart rate variability are related to less favorable responses to treatment[8,47]. In line with this, data from this study indicate that both the autonomic and immune systems may be involved in the effectiveness of neuromodulation therapy. Cardiac response during stimulation seems essential for improvement, but significant benefits are seen only when baseline inflammation is not elevated. These findings build on earlier research that connects vagal nerve function to immune and cardiovascular health.

Our findings suggest that WBC may be more relevant than CRP in moderating the relationship between HBC and clinical response. While CRP is a liver-derived acute-phase protein commonly used to track inflammation, WBC reflects the circulating burden of immune cells actively involved in initiating and sustaining inflammatory responses[25]. This includes cytokine secretion, a process directly linked to the immunomodulatory effects of the vagus nerve[28,29,33]. These biological differences (and WBC's closer alignment with vagal function) may help explain why only WBC moderated the relationship between HBC and treatment outcomes. Although prior studies have reported inconsistent associations between WBC and depression outcomes[48–51], these findings reconceptualize WBC as a moderator that conditions the clinical relevance of HBC. As such, WBC may serve as a cost-effective and scalable stratification marker, identifying individuals in whom HBC is more (or less) clinically informative. Finally, the moderation analysis further identified 6.44×10^9/L as the WBC threshold where this effect emerged. This value aligns with prior work linking WBC levels above $6\text{-}7 \times 10^9$/L to subclinical immune activation and increased risk for metabolic conditions[52,53] and all-cause mortality[54]. Although no consensus exists for defining low-grade inflammation by WBC in depression, individuals with values above 6×10^9/L show higher hospitalization rates than those with lower counts[55]. Together, these findings contextualize our threshold and support its clinical relevance. WBC appears to function both as a mechanistic moderator and a practical stratification tool, enhancing the clinical precision of HBC-guided neuromodulation in MDD.

Finally, FW imaging identified white matter alterations associated with elevated inflammation, providing structural evidence of reduced responsiveness to neuromodulation in limbic and prefrontal pathways implicated in affective and autonomic regulation. Patients with higher WBC levels exhibited increased FW in the fornix, corpus callosum, and, to a lesser extent, the

ATR. Elevated FW reflects an expansion of extracellular water and is widely regarded as a proxy for neuroinflammation[56,57]. The spatial distribution observed here aligns with circuits implicated in stress regulation, interoception, and autonomic control. The fornix, traditionally studied for its role in memory, also contributes to autonomic regulation as part of the limbic system and has been associated with allostatic load[58] and with therapeutic effects in MDD[57,59]. Increased FW in this tract may reflect disrupted hippocampal-hypothalamic signaling, consistent with reduced capacity for vagal engagement to promote homeostasis under conditions of elevated inflammation[58]. The ATR, which connects the anterior thalamus with prefrontal regions[60], is not typically considered part of classical autonomic circuits. However, recent evidence from deep-brain stimulation studies suggests that modulation of this tract can enhance HRV[61], pointing to an emerging role in autonomic regulation. Inflammation-related alterations in the ATR, as observed in various psychiatric disorders[62,63], may therefore impair the higher-order regulatory input required for HBC to exert clinical effects. The corpus callosum, though not a primary autonomic pathway, is highly sensitive to systemic stressors; both reduced HRV[64] and elevated inflammation[65] have been linked to compromised callosal integrity. Its involvement in the current findings suggests that immune-related disruption may also interfere with interhemispheric integration, further limiting the network flexibility necessary for effective neuromodulation. By demonstrating that peripheral immune activation is mirrored by microstructural changes in white matter tracts involved in autonomic and affective regulation, our FW results extend the moderating role of WBC beyond physiology into brain structure. This triad (i.e., elevated WBC, increased FW, and absent HBC benefit) may delineate a neuroimmune signature of reduced neuromodulation efficacy.

This study has several limitations. While WBC offers a practical index of systemic inflammation, it does not capture leukocyte subtypes or cytokines such as IL-6 and TNF-α, limiting insight into specific neuroimmune mechanisms relevant to depression and vagal signaling. Because WBC and HBC were measured only at baseline, their dynamic interplay remains unclear, and directionality between inflammation and vagal engagement cannot be determined. Although the sample was sufficiently powered to detect the WBC × HBC interaction (likelihood-ratio test power ≈ 80%), the null findings for CRP should be interpreted cautiously. Larger samples may also detect effects, especially at the higher inflammation levels, where we have only one participant who exceeded 10×10^9/L. Covariates such as BMI, especially in the case of CRP, were not systematically recorded and may have contributed to residual confounding. In addition, the use of single-shell DTI limits the biological specificity of free-water estimates, particularly in regions with complex fiber geometry[66,67]. Finally, in the context of our results, it is unclear whether the number of stimulation sessions in this protocol determined anti-inflammatory effects, particularly in participants with elevated baseline WBC.

CONCLUSION

In conclusion, this study shows that the clinical relevance of HBC during iTBS is shaped by systemic immune tone, as indexed by WBC. WBC distinguished patients with lower inflammation, in whom higher HBC was strongly associated with clinical benefit, whereas under higher inflammation, this discriminative value was lost. Diffusion MRI revealed inflammation-related white matter alterations in affective and autonomic circuits, linking peripheral immune tone to central neuroinflammatory processes. These findings position WBC as a practical stratification marker and highlight the importance of integrating immune and autonomic measures to enhance the precision and scalability of neuromodulatory treatments for depression. While this study focused on WBC to isolate physiological interactions with HBC, future research should adopt a longitudinal or systems-level approach (e.g., cytokine profiling) to refine mechanistic insight and advance biomarker-guided neuromodulation in MDD.

MATERIALS AND METHODS

Study design

We used data from the Pre-mapping Networks for Brain Stimulation 2 study (PreNeSt2, ClinicalTrials.gov identifier: NCT05260086), which investigated the neuromodulatory effects of iTBS in patients with MDD[68]. The parent study employed a six-week, quadruple-blind (participants, clinicians, investigators, and raters), randomized, sham-controlled, crossover design. Each participant underwent two stimulation interventions (one active and one sham) according to MATLAB-generated (The MathWorks, Inc., Natick, MA, USA) randomization order[68,69].

For the current analysis, psychometric data were used before crossover (week 1 to week 3), and the effect was quantified only during the first three weeks of the trial. In addition, we used baseline WBC, CRP, and HBC. As such, all HBC-related analyses are active stimulation with (higher) HBC, sham stimulation without HBC with participants randomized in between weeks 1 and 3, first 3 or 4 stimulations to be used to predict clinical benefit according to their HBC. Depression severity was assessed at baseline and after each treatment week using the Montgomery-Åsberg Depression Rating Scale (MADRS), administered by trained clinical interviewers [68,69].

Participants

All procedures conformed to the Declaration of Helsinki and were approved by the Ethics Committee of the University Medical Center Göttingen. Written and verbal informed consent was obtained from all participants before enrollment[70].

In the study, eligible participants were adults between 18 and 65 years old who met the DSM-5 criteria for MDD and were in a moderate to severe depressive episode. All diagnoses were confirmed by board-certified psychiatrists using the Structured Clinical Interview for DSM-5 Disorders - Clinical Version (SCID-5-CV) [69,71,72].

General exclusion criteria comprised any standard contraindications to rTMS, such as a personal history of epilepsy or seizures, significant neurological disease, pregnancy, or metallic implants incompatible with MRI or TMS[70].

For the analyses involving inflammatory markers, participants with laboratory evidence of acute or systemic inflammation at baseline were excluded. This was defined as CRP levels above 10 mg/L or WBC counts exceeding 11×10^9/L, based on routine clinical blood work[73,74].

All included individuals (n = 64) maintained a stable psychopharmacological regimen for at least two weeks before enrollment and throughout the intervention period. General characteristics of the sample are described in **Table 1 (see full sample)**.

iTBS treatment

The technical execution of the iTBS protocol adhered to the parameters outlined in the published trial protocol[68,69]. Treatment was administered with a MagVenture MagPro X100 system equipped with MagOption and a figure-of-eight MCF-B65 A/P cooled coil. All sessions were conducted by personnel trained in neuromodulation procedures.

Each treatment day comprised four iTBS sessions, each lasting approximately 10 minutes, with inter-session intervals of at least 20 minutes, consistent with the spaced stimulation approach supported by prior work[69,75]. Stimulation used the canonical iTBS pattern: bursts of three pulses at 50 Hz, repeated at 5 Hz, delivered for 2 seconds, followed by an 8-second pause. Each session delivered 60 bursts (1,800 pulses), totaling 7,200 pulses/day and 36,000 pulses/week.

The resting motor threshold (RMT) was established daily by surface electromyography of the right first dorsal interosseous muscle. RMT was defined as the minimum stimulator output that produced motor-evoked potentials ≥50 μV in at least 5 out of 10 consecutive trials. Stimulation intensity was set at 110% RMT.

Sham stimulation was delivered using the same coil rotated 180°, producing similar acoustic sensations without effective cortical stimulation. Additionally, transcutaneous electrical nerve stimulation electrodes were applied to the scalp during both active and sham sessions to replicate the cutaneous sensations of active TMS. The adequacy of blinding was evaluated post-intervention using a visual analogue scale[70].

Collections and assessment of CRP and WBC

Peripheral venous blood samples were collected from all participants at baseline, before allocation to treatment groups (active-sham, sham-active). Baseline inflammatory status was assessed from WBC and CRP levels.

CRP Measurement. Plasma CRP concentrations were measured from blood collected in lithium-heparin tubes using the Tina-quant C-Reactive Protein IV particle-enhanced immunoturbidimetric assay (Roche Diagnostics) on cobas c series clinical chemistry analyzers (c 303, c 503, c 703). Quantification was based on agglutination of latex microparticles coated with anti-CRP antibodies, with turbidity measured bichromatically at 570/800 nm. The assay had a validated range of 0.6-350 mg/L, a detection limit of 0.3 mg/L, and calibration traceable to ERM-DA474/IFCC. Analytical precision was maintained using two-level internal quality controls (within-run CV: 0.5-2.5%).

WBC Measurement. Total WBC counts were obtained from whole blood collected in 3 mL EDTA tubes using a Sysmex XN-series hematology analyzer (Sysmex, Kobe, Japan). The analyzer employed hydrodynamic focusing and a 663 nm semiconductor laser to measure forward scatter, side scatter, and side fluorescence signals, enabling assessment of cell size, internal

complexity, and nucleic acid content. Absolute counts were derived in the White-cell/Nucleated-RBC (WNR) channel following selective erythrocyte lysis and fluorescent staining of intracellular nucleic acids. This volumetric counting method requires no end-user calibration and provides precise leukocyte quantification for clinical and research use.

Heart-Brain-Coupling analysis

Electrocardiographic (ECG) data were processed using a custom-built analysis package in Python (Heart-Brain Coupling Toolbox; version 1.1; available at https://github.com/brainclinics/HBC). Detailed methodological specifications are provided elsewhere[22]. In cases where ECG artifacts were present, R-peaks were visually inspected and manually corrected using Kubios HRV software (version 4.1.0).

Briefly, R-peaks were first detected within the raw ECG recordings. The resulting heart rate (HR) time series was then convolved with a Hann window of 1.5 seconds to smooth the signal. Time-frequency representations were generated using the tfr_array_morlet function from the MNE-Python library, with a frequency range from 0.02 to 0.18 Hz in increments of 5×10^{-4} Hz. Analyses were performed with two different cycle settings: 3 cycles to maximize temporal resolution and 10 cycles to maximize frequency resolution.

To accommodate the analysis of low-frequency components, each dataset was zero-padded with the initial TMS block and rest period at the start, and the final block of data at the end. HBC was quantified by computing the mean spectral power (μV^2) at 0.1 Hz for iTBS datasets within each block and subsequently averaging these values across blocks. Final HBC values were adjusted for age and sex.

Statistical analysis

Although baseline WBC and CRP were strongly positively correlated in our sample, they were analyzed in separate moderation models for two reasons. First, from a biological perspective, total WBC reflects cellular immune status and is genetically linked to PSMD3 and CSF3, whereas CRP is a liver-derived acute-phase protein associated with HNF1A[25]. Each marker, therefore, indexes a distinct dimension of the inflammatory response. Second, from a statistical perspective, including two highly collinear predictors and their interaction terms in the same logistic model would inflate standard errors and obscure genuine effects due to multicollinearity. By testing WBC × HBC and CRP × HBC in parallel but independent models, we could isolate which facet of inflammation modulates the prognostic value of HBC without compromising model stability.

Following this, we tested whether baseline systemic inflammation moderated the relationship between early HBC during stimulation and clinical response to iTBS, defined as a ≥ 50% reduction in MADRS score from baseline to week 3[76]. Two separate logistic regression models were estimated, each including treatment allocation (active iTBS vs. sham), mean-centred

HBC (HBCc), one mean-centred inflammatory marker (either WBCc or CRPc), and the interaction term (HBCc × inflammatory marker). Model fit was assessed with Akaike information criterion (AIC), McFadden's pseudo-R^2, and Nagelkerke R^2. Likelihood-ratio tests evaluated main and interaction effects, and odds ratios (OR) with 95% confidence intervals (CI) were reported.

In cases where the moderation model reached significance, we validated model stability by computing nonparametric bias-corrected and accelerated (BCa) bootstrap confidence intervals with 1000 resamples. For each bootstrap iteration, regression coefficients were re-estimated and pseudo-R^2 statistics recalculated from log-likelihoods. Two-sided bootstrap p-values were obtained from the proportion of resamples crossing zero. This approach provided robust estimates of coefficients, confidence intervals, and effect sizes, thereby complementing classical maximum-likelihood inference.

Significant interactions were probed using simple-slope tests and the Johnson-Neyman technique to identify moderator ranges where HBC significantly predicted response. If an inflammatory parameter showed a significant interaction with HBC, it was carried forward to predictive modelling. In such cases, conditional marginal effects quantified the absolute change in response probability across levels of the moderator. For Receiver Operating Characteristic (ROC) analysis, participants were split according to the Johnson-Neyman bound of the significant inflammatory marker, and ROC curves were computed separately for each subgroup. Area under the curve (AUC) values with 95% CIs were calculated, and optimal thresholds were identified using the Youden index, with corresponding sensitivity, specificity, and classification accuracy. AUCs were tested against chance (0.50) using De Long's method.

All analyses and visualizations were conducted in R (version 4.4.3) via RStudio (version 12.1+563), with $\alpha = 0.05$ (two-tailed).

Free-water imaging analysis

As described above, significant interactions between inflammatory parameters and HBC were further examined using the Johnson-Neyman technique, which provided the exact moderator value at which the predictive effect of HBC on treatment response became significant. If an inflammatory marker (either CRP or WBC) showed a significant interaction, this threshold was then used to stratify participants into two subgroups: "higher" and "lower." These subgroups were subsequently carried forward to the FW imaging analyses to test whether inflammation-dependent differences in HBC were reflected in white matter microstructure.

To perform free-water imaging, diffusion MRI data from 64 participants were included in the connectometry database in DSI Studio (https://dsi-studio.labsolver.org). Scans were acquired using a diffusion tensor imaging (DTI) scheme with 63 sampling directions at a b-value of 1000 s/mm^2, with an isotropic resolution of $1.7mm^3$. Diffusion data were corrected for eddy current

and motion artifacts using FSL, with rotated b-vectors applied for subsequent analysis[77–79]. Images were resampled to an isotropic resolution of 2 mm, as the atlas platform shows greater compatibility with 2 mm than with 1.7 mm resolution. Integrity and quality checks were performed automatically[80] and visually inspected.

Diffusion data were reconstructed in MNI space using q-space diffeomorphic reconstruction (QSDR) to obtain the spin distribution function[66,81], with a diffusion sampling length ratio of 1.25 applied. To quantify FW from restricted diffusion, a bi-tensor model[82,83] was applied to separate partial volume effects and enhance sensitivity to tissue microstructure. To reduce partial volume effects and enhance sensitivity to tissue microstructure, FW correction was applied using a bi-tensor model[84,85]. The resulting FW values were extracted for connectometry analyses. Diffusion MRI connectometry[86] was then performed to assess parametric correlations between FW and the inflammatory marker, showing significant interactions (either CRP or WBC). As noted above, participants were divided into two groups based on the Johnson-Neyman analysis ("higher" or "lower" CRP; "higher" or "lower" WBC, depending on the modelling results) and analyzed separately for FW, revealing correlations with the respective parameter (CRP or WBC). An additional exploratory analysis directly compared the two subgroups to identify differences in FW, using nonparametric Spearman partial correlation.

All analyses conducted in DSI Studio used a multiple regression framework controlling for sex and age. Correlational tractography was performed using a deterministic fiber tracking algorithm[87]. Whole-brain seeding was employed, and a cerebellar mask was applied as a termination region. A T-score threshold of 3 was selected, and tracks were further refined using topology-informed pruning with four iterations[88]. Statistical significance was assessed using a false discovery rate (FDR) correction at $q < 0.05$, based on 8,000 randomized permutations.

BIBLIOGRAPHY

1. Dalhuisen, I. *et al*. rTMS as a Next Step in Antidepressant Nonresponders: A Randomized Comparison With Current Antidepressant Treatment Approaches. *Am. J. Psychiatry* **181**, 806–814 (2024).

2. Kishi, T. *et al*. Theta burst stimulation for depression: a systematic review and network and pairwise meta-analysis. *Mol. Psychiatry* **29**, 3893–3899 (2024).

3. Blumberger, D. M. *et al*. Effectiveness of theta burst versus high-frequency repetitive transcranial magnetic stimulation in patients with depression (THREE-D): a randomised non-inferiority trial. *The Lancet* **391**, 1683–1692 (2018).

4. Chung, S. W., Hoy, K. E. & Fitzgerald, P. B. Theta-burst stimulation: a new form of TMS treatment for depression? *Depress. Anxiety* **32**, 182–192 (2015).

5. Pérez-Castillo, I. M. *et al*. Does Lifelong Exercise Counteract Low-Grade Inflammation Associated with Aging? A Systematic Review and Meta-Analysis. *Sports Med*. **55**, 675–696 (2025).

6. Osimo, E. F., Baxter, L. J., Lewis, G., Jones, P. B. & Khandaker, G. M. Prevalence of low-grade inflammation in depression: a systematic review and meta-analysis of CRP levels. *Psychol. Med*. **49**, 1958–1970 (2019).

7. Rohleder, N. Stimulation of Systemic Low-Grade Inflammation by Psychosocial Stress. *Biopsychosoc. Sci. Med*. **76**, 181 (2014).

8. Beurel, E., Toups, M. & Nemeroff, C. B. The Bidirectional Relationship of Depression and Inflammation: Double Trouble. *Neuron* **107**, 234–256 (2020).

9. Suneson, K., Lindahl, J., Chamli Hårsmar, S., Söderberg, G. & Lindqvist, D. Inflammatory Depression—Mechanisms and Non-Pharmacological Interventions. *Int. J. Mol. Sci*. **22**, 1640 (2021).

10. Sohn, R. & Jenei-Lanzl, Z. Role of the Sympathetic Nervous System in Mild Chronic Inflammatory Diseases: Focus on Osteoarthritis. *Neuroimmunomodulation* **30**, 143–166 (2023).

11. Wu, Q., Miao, X., Cao, Y., Chi, A. & Xiao, T. Heart rate variability status at rest in adult depressed patients: a systematic review and meta-analysis. *Front. Public Health* **11**, (2023).

12. Di Biase, M. A. *et al*. Large-Scale Evidence for an Association Between Peripheral Inflammation and White Matter Free Water in Schizophrenia and Healthy Individuals. *Schizophr. Bull*. **47**, 542–551 (2021).

13. Langhein, M. *et al*. Association between peripheral inflammation and free-water imaging in Major Depressive Disorder before and after ketamine treatment - A pilot study. *J. Affect. Disord*. **314**, 78–85 (2022).

14. Kelly, S. *et al*. Widespread white matter microstructural differences in schizophrenia across 4322 individuals: results from the ENIGMA Schizophrenia DTI Working Group. *Mol. Psychiatry* **23**, 1261–1269 (2018).

15. Sun, Y. *et al*. Quantifying neuroinflammation within deep gray matter in small vessel disease using diffusion tensor based free-water imaging: a longitudinal study. *Front. Aging Neurosci.* **16**, (2024).

16. Troubat, R. *et al*. Neuroinflammation and depression: A review. *Eur. J. Neurosci.* **53**, 151–171 (2021).

17. Ay, I., Nasser, R., Simon, B. & Ay, H. Transcutaneous Cervical Vagus Nerve Stimulation Ameliorates Acute Ischemic Injury in Rats. *Brain Stimul. Basic Transl. Clin. Res. Neuromodulation* **9**, 166–173 (2016).

18. Zhou, L. *et al*. Neuroprotective effects of vagus nerve stimulation on traumatic brain injury. *Neural Regen. Res.* **9**, 1585 (2014).

19. Clough, R. W. *et al*. Cortical edema in moderate fluid percussion brain injury is attenuated by vagus nerve stimulation. *Neuroscience* **147**, 286–293 (2007).

20. Chen, Y. *et al*. Anti-neuroinflammation effects of transcutaneous auricular vagus nerve stimulation against depression-like behaviors via hypothalamic α7nAchR/JAK2/STAT3/NF-κB pathway in rats exposed to chronic unpredictable mild stress. *CNS Neurosci. Ther.* **29**, 2634–2644 (2023).

21. Dijkstra, E. *et al*. Transcranial Magnetic Stimulation–Induced Heart-Brain Coupling: Implications for Site Selection and Frontal Thresholding—Preliminary Findings. *Biol. Psychiatry Glob. Open Sci.* **3**, 939–947 (2023).

22. Iseger, T. A., Bueren, N. E. R. van, Kenemans, J. L., Gevirtz, R. & Arns, M. A frontal-vagal network theory for Major Depressive Disorder: Implications for optimizing neuromodulation techniques. *Brain Stimul. Basic Transl. Clin. Res. Neuromodulation* **13**, 1–9 (2020).

23. Iseger, T. A., Padberg, F., Kenemans, J. L., Gevirtz, R. & Arns, M. Neuro-Cardiac-Guided TMS (NCG-TMS): Probing DLPFC-sgACC-vagus nerve connectivity using heart rate – First results. *Brain Stimul. Basic Transl. Clin. Res. Neuromodulation* **10**, 1006–1008 (2017).

24. Pavlov, V. A. & Tracey, K. J. The vagus nerve and the inflammatory reflex—linking immunity and metabolism. *Nat. Rev. Endocrinol.* **8**, 743–754 (2012).

25. Kong, M. & Lee, C. Genetic associations with C-reactive protein level and white blood cell count in the KARE study. *Int. J. Immunogenet.* **40**, 120–125 (2013).

26. Willems, J. M., Trompet, S., Blauw, G. J., Westendorp, R. G. J. & de Craen, A. J. M. White Blood Cell Count and C-Reactive Protein Are Independent Predictors of Mortality in the Oldest Old. *J. Gerontol. Ser. A* **65A**, 764–768 (2010).

27. Dijkstra, E. S. A. *et al.* Probing prefrontal-sgACC connectivity using TMS-induced heart–brain coupling. *Nat. Ment. Health* **2**, 809–817 (2024).

28. Pavlov, V. A. & Tracey, K. J. The cholinergic anti-inflammatory pathway. *Brain. Behav. Immun.* **19**, 493–499 (2005).

29. Borovikova, L. V. *et al.* Vagus nerve stimulation attenuates the systemic inflammatory response to endotoxin. *Nature* **405**, 458–462 (2000).

30. Tracey, K. J. Physiology and immunology of the cholinergic antiinflammatory pathway. *J. Clin. Invest.* **117**, 289–296 (2007).

31. Adam, J., Rupprecht, S., Künstler, E. C. S. & Hoyer, D. Heart rate variability as a marker and predictor of inflammation, nosocomial infection, and sepsis – A systematic review. *Auton. Neurosci. Basic Clin.* **249**, (2023).

32. Shi, X. *et al.* Ameliorating effects and mechanisms of transcutaneous auricular vagal nerve stimulation on abdominal pain and constipation. *JCI Insight* **6**, (2021).

33. Lespérance, P. *et al.* Vagus Nerve Stimulation Modulates Inflammation in Treatment-Resistant Depression Patients: A Pilot Study. *Int. J. Mol. Sci.* **25**, 2679 (2024).

34. Williams, D. P. *et al.* Heart rate variability and inflammation: A meta-analysis of human studies. *Brain. Behav. Immun.* **80**, 219–226 (2019).

35. Ricon-Becker, I. *et al.* Tone it down: Vagal nerve activity is associated with pro-inflammatory and anti-viral factors in breast cancer – An exploratory study. *Compr. Psychoneuroendocrinology* **7**, 100057 (2021).

36. Kul'chyns'kyi, A. B., Kyjenko, V. M., Zukow, W. & Popovych, I. L. Causal Neuro-immune Relationships at Patients with Chronic Pyelonephritis and Cholecystitis. Correlations between Parameters EEG, HRV and White Blood Cell Count. *Open Med. Wars. Pol.* **12**, 201–213 (2017).

37. Thayer, J. F. & Sternberg, E. Beyond heart rate variability: vagal regulation of allostatic systems. *Ann. N. Y. Acad. Sci.* **1088**, 361–372 (2006).

38. Sproston, N. R. & Ashworth, J. J. Role of C-Reactive Protein at Sites of Inflammation and Infection. *Front. Immunol.* **9**, 754 (2018).

39. Benschop, R. J., Rodriguez-Feuerhahn, M. & Schedlowski, M. Catecholamine-induced leukocytosis: early observations, current research, and future directions. *Brain. Behav. Immun.* **10**, 77–91 (1996).

40. Ince, L. M., Weber, J. & Scheiermann, C. Control of Leukocyte Trafficking by Stress-Associated Hormones. *Front. Immunol.* **9**, (2019).

41. Kluft, C. & de Maat, M. P. Determination of the habitual low blood level of C-reactive protein in individuals. *Ital. Heart J. Off. J. Ital. Fed. Cardiol.* **2**, 172–180 (2001).

42. Bueno, H. *et al*. 2025 ESC Clinical Consensus Statement on mental health and cardiovascular disease: developed under the auspices of the ESC Clinical Practice Guidelines Committee: Developed by the task force on mental health and cardiovascular disease of the European Society of Cardiology (ESC)Endorsed by the European Federation of Psychologists' Associations AISBL (EFPA), the European Psychiatric Association (EPA), and the International Society of Behavioral Medicine (ISBM). *Eur. Heart J.* ehaf191 (2025) doi:10.1093/eurheartj/ehaf191.

43. Li, X., Zhou, J., Wang, M., Yang, C. & Sun, G. Cardiovascular disease and depression: a narrative review. *Front. Cardiovasc. Med.* **10**, (2023).

44. Lamadé, E. K. *et al*. Cardiovascular risk factors as potential biomarkers of length of hospital stay and rehospitalization in mood disorders – a retrospective study. *Biomark. Neuropsychiatry* **11**, 100109 (2024).

45. Galin, S. & Keren, H. The Predictive Potential of Heart Rate Variability for Depression. *Neuroscience* **546**, 88–103 (2024).

46. Sharif, S. *et al*. Low-grade inflammation as a risk factor for cardiovascular events and all-cause mortality in patients with type 2 diabetes. *Cardiovasc. Diabetol.* **20**, 220 (2021).

47. Suneson, K., Lindahl, J., Chamli Hårsmar, S., Söderberg, G. & Lindqvist, D. Inflammatory Depression—Mechanisms and Non-Pharmacological Interventions. *Int. J. Mol. Sci.* **22**, 1640 (2021).

48. Sealock, J. M. *et al*. Use of the PsycheMERGE Network to Investigate the Association Between Depression Polygenic Scores and White Blood Cell Count. *JAMA Psychiatry* **78**, 1365–1374 (2021).

49. Puangsri, P., Jinanarong, V. & Ninla-aesong, P. Impact of antidepressant treatment on complete blood count parameters and inflammatory ratios in adolescents with major depressive disorder. *J. Psychiatr. Res.* **157**, 26–35 (2023).

50. Wu, Q., Liu, J.-H., Ma, Q.-H., Xu, Y. & Pan, C.-W. White blood cell count as a mediator of the relationship between depressive symptoms and all-cause mortality: A community-based cohort study. *Arch. Gerontol. Geriatr.* **94**, 104343 (2021).

51. Cao, Y. *et al*. Revealing the Causal Relationship Between Differential White Blood Cell Counts and Depression: A Bidirectional Two-Sample Mendelian Randomization Study. *Depress. Anxiety* **2025**, 3131579 (2025).

52. Farhangi, M. A., Keshavarz, S.-A., Eshraghian, M., Ostadrahimi, A. & Saboor-Yaraghi, A.-A. White Blood Cell Count in Women: Relation to Inflammatory Biomarkers, Haematological Profiles, Visceral Adiposity, and Other Cardiovascular Risk Factors. *J. Health Popul. Nutr.* **31**, 58–64 (2013).

53. Twig, G. *et al*. White Blood Cells Count and Incidence of Type 2 Diabetes in Young Men. *Diabetes Care* **36**, 276–282 (2013).

54. Ruggiero, C. *et al*. White blood cell count and mortality in the Baltimore Longitudinal Study of Aging. *J. Am. Coll. Cardiol.* **49**, 1841–1850 (2007).

55. Köhler-Forsberg, O. *et al*. White blood cell count at first depression diagnosis as predictor for risk of subsequent hospitalization with depression. *Neurol. Psychiatry Brain Res.* **26**, 1–6 (2017).

56. Pasternak, O., Westin, C.-F., Dahlben, B., Bouix, S. & Kubicki, M. The extent of diffusion MRI markers of neuroinflammation and white matter deterioration in chronic schizophrenia. *Schizophr. Res.* **161**, 113–118 (2015).

57. Ning, L., Rathi, Y., Barbour, T., Makris, N. & Camprodon, J. A. White matter markers and predictors for subject-specific rTMS response in major depressive disorder. *J. Affect. Disord.* **299**, 207–214 (2022).

58. Savransky, A. *et al*. Fornix Structural Connectivity and Allostatic Load: Empirical Evidence From Schizophrenia Patients and Healthy Controls. *Biopsychosoc. Sci. Med.* **79**, 770 (2017).

59. Korgaonkar, M. S., Williams, L. M., Song, Y. J., Usherwood, T. & Grieve, S. M. Diffusion tensor imaging predictors of treatment outcomes in major depressive disorder. *Br. J. Psychiatry J. Ment. Sci.* **205**, 321–328 (2014).

60. Mamah, D. *et al*. Anterior thalamic radiation integrity in schizophrenia: A diffusion-tensor imaging study. *Psychiatry Res. Neuroimaging* **183**, 144–150 (2010).

61. Lőrincz, K. *et al*. Effects of anterior thalamic nucleus DBS on interictal heart rate variability in patients with refractory epilepsy. *Clin. Neurophysiol. Off. J. Int. Fed. Clin. Neurophysiol.* **147**, 17–30 (2023).

62. Niida, R. *et al*. Aberrant Anterior Thalamic Radiation Structure in Bipolar Disorder: A Diffusion Tensor Tractography Study. *Front. Psychiatry* **9**, (2018).

63. Cao, Y. *et al*. White matter microstructural and inflammation-based subgroups in bipolar disorder II depression differentiate in depressive and psychotic symptoms. *J. Affect. Disord.* **368**, 493–502 (2025).

64. Jiang, S. *et al*. Cognitive implications of white matter microstructural changes in individuals with low heart rate variability: a NODDI study. *Front. Neurol.* **16**, (2025).

65. Thomas, M. *et al*. Elevated Systemic Inflammation Is Associated with Reduced Corticolimbic White Matter Integrity in Depression. *Life* **12**, 43 (2022).

66. Yeh, F.-C. & Tseng, W.-Y. I. NTU-90: a high angular resolution brain atlas constructed by q-space diffeomorphic reconstruction. *NeuroImage* **58**, 91–99 (2011).

67. Golub, M., Neto Henriques, R. & Gouveia Nunes, R. Free-water DTI estimates from single b-value data might seem plausible but must be interpreted with care. *Magn. Reson. Med.* **85**, 2537–2551 (2021).

68. Wilkening, J., Witteler, F. & Goya-Maldonado, R. Suicidality and relief of depressive symptoms with intermittent theta burst stimulation in a sham-controlled randomized clinical trial. *Acta Psychiatr. Scand.* **146**, 540–556 (2022).

69. Wilkening, J. & Goya-Maldonado, R. White matter tracts associated with iTBS-induced heart rate deceleration and treatment response in major depressive disorder. 2025.01.09.25320274 Preprint at https://doi.org/10.1101/2025.01.09.25320274 (2025).

70. Wilkening, J. *et al.* Heart Rate Modulation and Clinical Improvement in Major Depression: A Randomized Clinical Trial with Accelerated Intermittent Theta Burst Stimulation. 2025.04.06.25325324 Preprint at https://doi.org/10.1101/2025.04.06.25325324 (2025).

71. Hengartner, M. P., Jakobsen, J. C., Sørensen, A. & Plöderl, M. Efficacy of new-generation antidepressants assessed with the Montgomery-Asberg Depression Rating Scale, the gold standard clinician rating scale: A meta-analysis of randomised placebo-controlled trials. *PLOS ONE* **15**, e0229381 (2020).

72. Montgomery, S. A. & Åsberg, M. A New Depression Scale Designed to be Sensitive to Change. *Br. J. Psychiatry* **134**, 382–389 (1979).

73. Chmielewski, P. P. & Strzelec, B. Elevated leukocyte count as a harbinger of systemic inflammation, disease progression, and poor prognosis: a review. *Folia Morphol.* **77**, 171–178 (2018).

74. Lelubre, C., Anselin, S., Zouaoui Boudjeltia, K., Biston, P. & Piagnerelli, M. Interpretation of C-Reactive Protein Concentrations in Critically Ill Patients. *BioMed Res. Int.* **2013**, 124021 (2013).

75. Tse, N. Y. *et al.* The effect of stimulation interval on plasticity following repeated blocks of intermittent theta burst stimulation. *Sci. Rep.* **8**, 8526 (2018).

76. Trivedi, M. H. *et al.* Remission, response without remission, and nonresponse in major depressive disorder: impact on functioning. *Int. Clin. Psychopharmacol.* **24**, 133 (2009).

77. Andersson, J. L. R. & Sotiropoulos, S. N. An integrated approach to correction for off-resonance effects and subject movement in diffusion MR imaging. *NeuroImage* **125**, 1063–1078 (2016).

78. Jenkinson, M., Beckmann, C. F., Behrens, T. E. J., Woolrich, M. W. & Smith, S. M. FSL. *NeuroImage* **62**, 782–790 (2012).

79. Leemans, A. & Jones, D. K. The B-matrix must be rotated when correcting for subject motion in DTI data. *Magn. Reson. Med.* **61**, 1336–1349 (2009).

80. Yeh, F.-C. *et al.* Differential tractography as a track-based biomarker for neuronal injury. *NeuroImage* **202**, 116131 (2019).

81. Yeh, F.-C., Wedeen, V. J. & Tseng, W.-Y. I. Generalized q-sampling imaging. *IEEE Trans. Med. Imaging* **29**, 1626–1635 (2010).

82. Hoy, A. R., Koay, C. G., Kecskemeti, S. R. & Alexander, A. L. Optimization of a free water elimination two-compartment model for diffusion tensor imaging. *NeuroImage* **103**, 323–333 (2014).

83. Pasternak, O., Sochen, N., Gur, Y., Intrator, N. & Assaf, Y. Free water elimination and mapping from diffusion MRI. *Magn. Reson. Med.* **62**, 717–730 (2009).

84. Hoy, A. R., Koay, C. G., Kecskemeti, S. R. & Alexander, A. L. Optimization of a free water elimination two-compartment model for diffusion tensor imaging. *NeuroImage* **103**, 323–333 (2014).

85. Pasternak, O., Sochen, N., Gur, Y., Intrator, N. & Assaf, Y. Free water elimination and mapping from diffusion MRI. *Magn. Reson. Med.* **62**, 717–730 (2009).

86. Yeh, F.-C., Badre, D. & Verstynen, T. Connectometry: A statistical approach harnessing the analytical potential of the local connectome. *NeuroImage* **125**, 162–171 (2016).

87. Yeh, F.-C., Tang, P.-F. & Tseng, W.-Y. I. Diffusion MRI connectometry automatically reveals affected fiber pathways in individuals with chronic stroke. *NeuroImage Clin.* **2**, 912–921 (2013).

88. Yeh, F.-C. *et al.* Automatic Removal of False Connections in Diffusion MRI Tractography Using Topology-Informed Pruning (TIP). *Neurother. J. Am. Soc. Exp. Neurother.* **16**, 52–58 (2019).